Evidence for $e^+e^- \to \gamma\chi_{c1,2}$ at center-of-mass energies from 4.009 to 4.360 GeV

2015 Chinese Phys. C 39 041001

(http://iopscience.iop.org/1674-1137/39/4/041001)

Evidence for $e^+e^- \to \gamma\chi_{c1,2}$ at center-of-mass energies from 4.009 to 4.360 GeV*

M. Ablikim(麦迪娜)[1] M. N. Achasov[8,a] X. C. Ai(艾小聪)[1] O. Albayrak[4] M. Albrecht[3] D. J. Ambrose[43] A. Amoroso[47A,47C] F. F. An(安芬芬)[1] Q. An(安琪)[44] J. Z. Bai(白景芝)[1] R. Baldini Ferroli[19A] Y. Ban(班勇)[30] D. W. Bennett[18] J. V. Bennett[4] M. Bertani[19A] D. Bettoni[20A] J. M. Bian(边渐鸣)[42] F. Bianchi[47A,47C] E. Boger[22,h] O. Bondarenko[24] I. Boyko[22] R. A. Briere[4] H. Cai(蔡浩)[49] X. Cai(蔡啸)[1] O. Cakir[39A,b] A. Calcaterra[19A] G. F. Cao(曹国富)[1] S. A. Cetin[39B] J. F. Chang(常劲帆)[1] G. Chelkov[22,c] G. Chen(陈刚)[1] H. S. Chen(陈和生)[1] H. Y. Chen(陈海云)[2] J. C. Chen(陈江川)[1] M. L. Chen(陈玛丽)[1] S. J. Chen(陈申见)[28] X. Chen(谌炫)[1] X. R. Chen(陈旭荣)[25] Y. B. Chen(陈元柏)[1] H. P. Cheng(程和平)[16] X. K. Chu(褚新坤)[30] G. Cibinetto[20A] D. Cronin-Hennessy[42] H. L. Dai(代洪亮)[1] J. P. Dai(代建平)[33] A. Dbeyssi[13] D. Dedovich[22] Z. Y. Deng(邓子艳)[1] A. Denig[21] I. Denysenko[22] M. Destefanis[47A,47C] F. De Mori[47A,47C] Y. Ding(丁勇)[26] C. Dong(董超)[29] J. Dong(董静)[1] L. Y. Dong(董燎原)[1] M. Y. Dong(董明义)[1] S. X. Du(杜书先)[51] P. F. Duan(段鹏飞)[1] J. Z. Fan(范荆州)[38] J. Fang(方建)[1] S. S. Fang(房双世)[1] X. Fang(方馨)[44] Y. Fang(方易)[1] L. Fava[47B,47C] F. Feldbauer[21] G. Felici[19A] C. Q. Feng(封常青)[44] E. Fioravanti[20A] M. Fritsch[13,21] C. D. Fu(傅成栋)[1] Q. Gao(高清)[1] Y. Gao(高原宁)[38] Z. Gao(高榛)[44] I. Garzia[20A] K. Goetzen[9] W. X. Gong(龚文煊)[1] W. Gradl[21] M. Greco[47A,47C] M. H. Gu(顾旻皓)[1] Y. T. Gu(顾运厅)[11] Y. H. Guan(管颖慧)[1] A. Q. Guo(郭爱强)[1] L. B. Guo(郭立波)[27] T. Guo(郭暾)[27] Y. Guo(郭玥)[1] Y. P. Guo[21] Z. Haddadi[24] A. Hafner[21] S. Han(韩爽)[49] Y. L. Han(韩艳良)[1] F. A. Harris[41] K. L. He(何康林)[1] Z. Y. He(何振亚)[29] T. Held[3] Y. K. Heng(衡月昆)[1] Z. L. Hou(侯治龙)[1] C. Hu(胡琛)[27] H. M. Hu(胡海明)[1] J. F. Hu(胡继峰)[47A] T. Hu(胡涛)[1] Y. Hu(胡誉)[1] G. M. Huang(黄光明)[5] G. S. Huang(黄光顺)[44] H. P. Huang(黄海鹏)[49] J. S. Huang(黄金书)[14] X. T. Huang(黄性涛)[32] Y. Huang(黄勇)[28] T. Hussain[46] Q. Ji(纪全)[1] Q. P. Ji(姬清平)[29] X. B. Ji(季晓斌)[1] X. L. Ji(季筱璐)[1] L. L. Jiang(姜丽丽)[1] L. W. Jiang(姜鲁文)[49] X. S. Jiang(江晓山)[1] J. B. Jiao(焦健斌)[32] Z. Jiao(焦铮)[16] D. P. Jin(金大鹏)[1] S. Jin(金山)[1] T. Johansson[48] A. Julin[42] N. Kalantar-Nayestanaki[24] X. L. Kang(康晓琳)[1] X. S. Kang(康晓珅)[29] M. Kavatsyuk[24] B. C. Ke[4] R. Kliemt[13] B. Kloss[21] O. B. Kolcu[39B,d] B. Kopf[3] M. Kornicer[41] W. Kuehn[23] A. Kupsc[48] W. Lai(赖蔚)[1] J. S. Lange[23] M. Lara[18] P. Larin[13] C. H. Li(李春花)[1] Cheng Li(李澄)[44] D. M. Li(李德民)[51] F. Li(李飞)[1] G. Li(李刚)[1] H. B. Li(李海波)[1] J. C. Li(李家才)[1] Jin Li(李瑾)[31] K. Li(李康)[12] K. Li(李科)[32] P. R. Li(李培荣)[40] T. Li(李腾)[32] W. D. Li(李卫东)[1] W. G. Li(李卫国)[1] X. L. Li(李晓玲)[32] X. M. Li(李小梅)[11] X. N. Li(李小男)[1] X. Q. Li(李学潜)[29] Z. B. Li(李志兵)[37] H. Liang(梁昊)[44] Y. F. Liang(梁勇飞)[35] Y. T. Liang(梁羽铁)[23] G. R. Liao(廖广睿)[10] D. X. Lin(Lin)[13] B. J. Liu(刘北江)[1] C. L. Liu[4] C. X. Liu(刘春秀)[1] F. H. Liu(刘福虎)[34] Fang Liu(刘芳)[1] Feng Liu(刘峰)[5] H. B. Liu(刘宏邦)[11] H. H. Liu(刘汇慧)[15]

Received 25 October 2014

∗Supported by National Key Basic Research Program of China (2015CB856700), Joint Funds of National Natural Science Foundation of China (11079008, 11179007, U1232201, U1332201, U1232107), National Natural Science Foundation of China (NSFC) (10935007, 11121092, 11125525, 11235011, 11322544, 11335008), Chinese Academy of Sciences (CAS) Large-Scale Scientific Facility Program, CAS (KJCX2-YW-N29, KJCX2-YW-N45), 100 Talents Program of CAS, INPAC and Shanghai Key Laboratory for Particle Physics and Cosmology; German Research Foundation DFG (Collaborative Research Center CRC-1044), Istituto Nazionale di Fisica Nucleare, Italy, Ministry of Development of Turkey (DPT2006K-120470), Russian Foundation for Basic Research (14-07-91152), U. S. Department of Energy (DE-FG02-04ER41291, DE-FG02-05ER41374, DE-FG02-94ER40823, DESC0010118), U.S. National Science Foundation, University of Groningen (RuG) and Helmholtzzentrum fuer Schwerionenforschung GmbH (GSI), Darmstadt, WCU Program of National Research Foundation of Korea (R32-2008-000-10155-0)

H. H. Liu(刘欢欢)[1] H. M. Liu(刘怀民)[1] J. Liu(刘杰)[1] J. P. Liu(刘觉平)[49] J. Y. Liu(刘晶译)[1]
K. Liu(刘凯)[38] K. Y. Liu(刘魁勇)[26] L. D. Liu(刘兰雕)[30] P. L. Liu(刘佩莲)[1] Q. Liu(刘倩)[40]
S. B. Liu(刘树彬)[44] X. Liu(刘翔)[25] X. X. Liu(刘晓霞)[40] Y. B. Liu(刘玉斌)[29] Z. A. Liu(刘振安)[1]
Zhiqiang Liu(刘志强)[1] Zhiqing Liu[21] H. Loehner[24] X. C. Lou(娄辛丑)[1,e] H. J. Lu(吕海江)[16]
J. G. Lu(吕军光)[1] R. Q. Lu(鲁睿其)[17] Y. Lu(卢宇)[1] Y. P. Lu(卢云鹏)[1] C. L. Luo(罗成林)[27]
M. X. Luo(罗民兴)[50] T. Luo[41] X. L. Luo(罗小兰)[1] M. Lv(吕蒙)[1] X. R. Lyu(吕晓睿)[40] F. C. Ma(马凤才)[26]
H. L. Ma(马海龙)[1] L. L. Ma(马连良)[32] Q. M. Ma(马秋梅)[1] S. Ma(马斯)[1] T. Ma(马天)[1] X. N. Ma(马旭宁)[29]
X. Y. Ma(马骁妍)[1] F. E. Maas[13] M. Maggiora[47A,47C] Q. A. Malik[46] Y. J. Mao(冒亚军)[30] Z. P. Mao(毛泽普)[1]
S. Marcello[47A,47C] J. G. Messchendorp[24] J. Min(闵建)[1] T. J. Min(闵天觉)[1] R. E. Mitchell[18]
X. H. Mo(莫晓虎)[1] Y. J. Mo(莫玉俊)[5] C. Morales Morales[13] K. Moriya[18] N. Yu. Muchnoi[8,a] H. Muramatsu[42]
Y. Nefedov[22] F. Nerling[13] I. B. Nikolaev[8,a] Z. Ning(宁哲)[1] S. Nisar[7] S. L. Niu(牛顺利)[1] X. Y. Niu(牛讯伊)[1]
S. L. Olsen(馬鵬)[31] Q. Ouyang(欧阳群)[1] S. Pacetti[19B] P. Patteri[19A] M. Pelizaeus[3] H. P. Peng(彭海平)[44]
K. Peters[9] J. L. Ping(平加伦)[27] R. G. Ping(平荣刚)[1] R. Poling[42] Y. N. Pu(濮亚男)[17] M. Qi(祁鸣)[28]
S. Qian(钱森)[1] C. F. Qiao(乔从丰)[40] L. Q. Qin(秦丽清)[32] N. Qin(覃拈)[49] X. S. Qin(秦小帅)[1] Y. Qin(秦瑶)[30]
Z. H. Qin(秦中华)[1] J. F. Qiu(邱进发)[1] K. H. Rashid[46] C. F. Redmer[21] H. L. Ren(任海龙)[17] M. Ripka[21]
G. Rong(荣刚)[1] X. D. Ruan(阮向东)[11] V. Santoro[20A] A. Sarantsev[22,f] M. Savrié[20B] K. Schoenning[48]
S. Schumann[21] W. Shan(单葳)[30] M. Shao(邵明)[44] C. P. Shen(沈成平)[2] P. X. Shen(沈培迅)[29]
X. Y. Shen(沈肖雁)[1] H. Y. Sheng(盛华义)[1] M. R. Shepherd[18] W. M. Song(宋维民)[1] X. Y. Song(宋欣颖)[1]
S. Sosio[47A,47C] S. Spataro[47A,47C] B. Spruck[23] G. X. Sun(孙功星)[1] J. F. Sun(孙俊峰)[14] S. S. Sun(孙胜森)[1]
Y. J. Sun(孙勇杰)[44] Y. Z. Sun(孙永昭)[1] Z. J. Sun(孙志嘉)[1] Z. T. Sun(孙振田)[18] C. J. Tang(唐昌建)[35]
X. Tang(唐晓)[1] I. Tapan[39C] E. H. Thorndike[43] M. Tiemens[24] D. Toth[42] M. Ullrich[23] I. Uman[39B]
G. S. Varner[41] B. Wang(王斌)[29] B. L. Wang(王滨龙)[40] D. Wang(王东)[30] D. Y. Wang(王大勇)[30]
K. Wang(王科)[1] L. L. Wang(王亮亮)[1] L. S. Wang(王灵淑)[1] M. Wang(王萌)[32] P. Wang(王平)[1]
P. L. Wang(王佩良)[1] Q. J. Wang(王庆娟)[1] S. G. Wang(王思广)[30] W. Wang(王炜)[1] X. F. Wang(王雄飞)[38]
Y. D. Wang(Yadi)[19A] Y. F. Wang(王贻芳)[1] Y. Q. Wang(王亚乾)[21] Z. Wang(王铮)[1] Z. G. Wang(王志刚)[1]
Z. H. Wang(王志宏)[44] Z. Y. Wang(王至勇)[1] T. Weber[21] D. H. Wei(魏代会)[10] J. B. Wei(韦江波)[30]
P. Weidenkaff[21] S. P. Wen(文硕频)[1] U. Wiedner[3] M. Wolke[48] L. H. Wu(伍灵慧)[1] Z. Wu(吴智)[1]
L. G. Xia(夏力钢)[38] Y. Xia(夏宇)[17] D. Xiao(肖栋)[1] Z. J. Xiao(肖振军)[27] Y. G. Xie(谢宇广)[1]
G. F. Xu(许国发)[1] L. Xu(徐雷)[1] Q. J. Xu(徐庆君)[12] Q. N. Xu(徐庆年)[40] X. P. Xu(徐新平)[36]
L. Yan(严亮)[44] W. B. Yan(鄢文标)[44] W. C. Yan(闫文成)[44] Y. H. Yan(颜永红)[17] H. X. Yang(杨洪勋)[1]
L. Yang(杨柳)[49] Y. Yang(杨迎)[5] Y. X. Yang(杨永栩)[10] H. Ye(叶桦)[1] M. Ye(叶梅)[1] M. H. Ye(叶铭汉)[6]
J. H. Yin(殷俊昊)[1] B. X. Yu(俞伯祥)[1] C. X. Yu(喻纯旭)[29] H. W. Yu(于海旺)[30] J. S. Yu(俞洁晟)[25]
C. Z. Yuan(苑长征)[1] W. L. Yuan(袁文龙)[28] Y. Yuan(袁野)[1] A. Yuncu[39B,g] A. A. Zafar[46] A. Zallo[19A]
Y. Zeng(曾云)[17] B. X. Zhang(张丙新)[1] B. Y. Zhang(张炳云)[1] C. Zhang(张驰)[28] C. C. Zhang(张长春)[1]
D. H. Zhang(张达华)[1] H. H. Zhang(张宏浩)[37] H. Y. Zhang(章红宇)[1] J. J. Zhang(张佳佳)[1]
J. L. Zhang(张杰磊)[1] J. Q. Zhang(张敬庆)[1] J. W. Zhang(张家文)[1] J. Y. Zhang(张建勇)[1]
J. Z. Zhang(张景芝)[1] K. Zhang(张坤)[1] L. Zhang(张磊)[1] S. H. Zhang(张书华)[1] X. Y. Zhang(张学尧)[32]
Y. Zhang(张瑶)[1] Y. H. Zhang(张银鸿)[1] Y. T. Zhang(张亚腾)[44] Z. H. Zhang(张正好)[5]
Z. P. Zhang(张子平)[44] Z. Y. Zhang(张振宇)[49] G. Zhao(赵光)[1] J. W. Zhao(赵京伟)[1] J. Y. Zhao(赵静宜)[1]
J. Z. Zhao(赵京周)[1] Lei Zhao(赵雷)[44] Ling Zhao(赵玲)[1] M. G. Zhao(赵明刚)[29] Q. Zhao(赵强)[1]
Q. W. Zhao(赵庆旺)[1] S. J. Zhao(赵书俊)[51] T. C. Zhao(赵天池)[1] Y. B. Zhao(赵豫斌)[1] Z. G. Zhao(赵政国)[44]
A. Zhemchugov[22,h] B. Zheng(郑波)[45] J. P. Zheng(郑建平)[1] W. J. Zheng(郑文静)[32] Y. H. Zheng(郑阳恒)[40]
B. Zhong(钟彬)[27] L. Zhou(周莉)[1] Li Zhou(周立)[29] X. Zhou(周详)[49] X. K. Zhou(周晓康)[44]
X. R. Zhou(周小蓉)[44] X. Y. Zhou(周兴玉)[1] K. Zhu(朱凯)[1] K. J. Zhu(朱科军)[1] S. Zhu(朱帅)[1]
X. L. Zhu(朱相雷)[38] Y. C. Zhu(朱莹春)[44] Y. S. Zhu(朱永生)[1] Z. A. Zhu(朱自安)[1]

J. Zhuang(庄建)[1] B. S. Zou(邹冰松)[1] J. H. Zou(邹佳恒)[1]
(BESIII collaboration)

[1] Institute of High Energy Physics, Chinese Academy of Sciences, Beijing 100049, China
[2] Beihang University, Beijing 100191, China
[3] Bochum Ruhr-University, D-44780 Bochum, Germany
[4] Carnegie Mellon University, Pittsburgh, Pennsylvania 15213, USA
[5] Central China Normal University, Wuhan 430079, China
[6] China Center of Advanced Science and Technology, Beijing 100190, China
[7] COMSATS Institute of Information Technology, Lahore, Defence Road, Off Raiwind Road, 54000 Lahore, Pakistan
[8] G.I. Budker Institute of Nuclear Physics SB RAS (BINP), Novosibirsk 630090, Russia
[9] GSI Helmholtzcentre for Heavy Ion Research GmbH, D-64291 Darmstadt, Germany
[10] Guangxi Normal University, Guilin 541004, China
[11] Guangxi University, Nanning 530004, China
[12] Hangzhou Normal University, Hangzhou 310036, China
[13] Helmholtz Institute Mainz, Johann-Joachim-Becher-Weg 45, D-55099 Mainz, Germany
[14] Henan Normal University, Xinxiang 453007, China
[15] Henan University of Science and Technology, Luoyang 471003, China
[16] Huangshan College, Huangshan 245000, China
[17] Hunan University, Changsha 410082, China
[18] Indiana University, Bloomington, Indiana 47405, USA
[19] (A)INFN Laboratori Nazionali di Frascati, I-00044, Frascati, Italy; (B)INFN and University of Perugia, I-06100, Perugia, Italy
[20] (A)INFN Sezione di Ferrara, I-44122, Ferrara, Italy; (B)University of Ferrara, I-44122, Ferrara, Italy
[21] Johannes Gutenberg University of Mainz, Johann-Joachim-Becher-Weg 45, D-55099 Mainz, Germany
[22] Joint Institute for Nuclear Research, 141980 Dubna, Moscow region, Russia
[23] Justus Liebig University Giessen, II. Physikalisches Institut, Heinrich-Buff-Ring 16, D-35392 Giessen, Germany
[24] KVI-CART, University of Groningen, NL-9747 AA Groningen, The Netherlands
[25] Lanzhou University, Lanzhou 730000, China
[26] Liaoning University, Shenyang 110036, China
[27] Nanjing Normal University, Nanjing 210023, China
[28] Nanjing University, Nanjing 210093, China
[29] Nankai University, Tianjin 300071, China
[30] Peking University, Beijing 100871, China
[31] Seoul National University, Seoul, 151-747 Korea
[32] Shandong University, Jinan 250100, China
[33] Shanghai Jiao Tong University, Shanghai 200240, China
[34] Shanxi University, Taiyuan 030006, China
[35] Sichuan University, Chengdu 610064, China
[36] Soochow University, Suzhou 215006, China
[37] Sun Yat-Sen University, Guangzhou 510275, China
[38] Tsinghua University, Beijing 100084, China
[39] (A)Istanbul Aydin University, 34295 Sefakoy, Istanbul, Turkey; (B)Dogus University, 34722 Istanbul, Turkey; (C)Uludag University, 16059 Bursa, Turkey
[40] University of Chinese Academy of Sciences, Beijing 100049, China
[41] University of Hawaii, Honolulu, Hawaii 96822, USA
[42] University of Minnesota, Minneapolis, Minnesota 55455, USA
[43] University of Rochester, Rochester, New York 14627, USA
[44] University of Science and Technology of China, Hefei 230026, China
[45] University of South China, Hengyang 421001, China
[46] University of the Punjab, Lahore-54590, Pakistan
[47] (A)University of Turin, I-10125, Turin, Italy; (B)University of Eastern Piedmont, I-15121, Alessandria, Italy; (C)INFN, I-10125, Turin, Italy
[48] Uppsala University, Box 516, SE-75120 Uppsala, Sweden
[49] Wuhan University, Wuhan 430072, China
[50] Zhejiang University, Hangzhou 310027, China
[51] Zhengzhou University, Zhengzhou 450001, China
[a] Also at the Novosibirsk State University, Novosibirsk, 630090, Russia
[b] Also at Ankara University, 06100 Tandogan, Ankara, Turkey
[c] Also at the Moscow Institute of Physics and Technology, Moscow 141700, Russia and at the Functional Electronics Laboratory, Tomsk State University, Tomsk, 634050, Russia
[d] Currently at Istanbul Arel University, Kucukcekmece, Istanbul, Turkey
[e] Also at University of Texas at Dallas, Richardson, Texas 75083, USA
[f] Also at the PNPI, Gatchina 188300, Russia
[g] Also at Bogazici University, 34342 Istanbul, Turkey
[h] Also at the Moscow Institute of Physics and Technology, Moscow 141700, Russia

Abstract: Using data samples collected at center-of-mass energies of $\sqrt{s}$=4.009, 4.230, 4.260, and 4.360 GeV with the BESIII detector operating at the BEPC II collider, we perform a search for the process $e^+e^-\to\gamma\chi_{cJ}$ (J=0, 1, 2)

and find evidence for $e^+e^-\to\gamma\chi_{c1}$ and $e^+e^-\to\gamma\chi_{c2}$ with statistical significances of 3.0σ and 3.4σ, respectively. The Born cross sections $\sigma^{\rm B}(e^+e^-\to\gamma\chi_{cJ})$, as well as their upper limits at the 90% confidence level (C.L.) are determined at each center-of-mass energy.

Key words: heavy quarkonia, decays of hadronic, electron-positron collisions, hadron production by

PACS: 14.40.Pq, 13.25.Gv, 13.66.Bc **DOI:** 10.1088/1674-1137/39/4/041001

1 Introduction

The charmonium-like state Y(4260) was first observed in the initial state radiation (ISR) process $e^+e^-\to\gamma_{\rm ISR}\pi^+\pi^-J/\psi$ by BaBar [1], and later confirmed by the CLEO [2] and Belle [3] experiments. Recently, both BaBar and Belle updated their results with full data sets, and further confirmed the existence of the Y(4260) [4, 5]. Since it is produced through ISR in e^+e^- annihilation, the Y(4260) has the quantum numbers $J^{PC}=1^{--}$. However, there seems to be no $c\bar{c}$ slot available for the Y(4260) in the conventional charmonium family [6]. In addition, a number of unusual features, such as a strong coupling to hidden-charm final states, suggest that the Y(4260) is a non-conventional $c\bar{c}$ meson. Possible interpretations of this state can be found in Refs. [7–11], but all need further experimental input.

Most of the previous studies of the Y(4260) have utilized hadronic transitions. Except for the clear signal observed in the $\pi^+\pi^-J/\psi$ decay mode, the Belle experiment failed to find evidence of the Y(4260) via the $e^+e^-\to\gamma_{\rm ISR}\eta J/\psi$ process [12]. Based on 13.2 $\rm pb^{-1}$ of e^+e^- data collected at $\sqrt{s}=4.260$ GeV, the CLEO experiment investigated fourteen hadronic decay channels, but the only charmonium channels with more than 3σ statistical significance are $\pi^+\pi^-J/\psi$, $\pi^0\pi^0J/\psi$ and K^+K^-J/ψ [13]. The BESIII Collaboration first observed the process $e^+e^-\to\gamma X(3872)$ using data samples taken between $\sqrt{s}=4.009$ and 4.420 GeV [14], which strongly supports the existence of the radiative transition decays of the Y(4260). To further understand the nature of the Y(4260) state, an investigation into the radiative transitions between the Y(4260) and other lower mass charmonium states, like the χ_{cJ} ($J=0$, 1, 2), is important [15, 16]. The cross sections of $e^+e^-\to\gamma\chi_{cJ}$ have been evaluated theoretically within the framework of non-relativistic quantum chromodynamics (NRQCD) [16]. Experimentally, the only existing investigation comes from the CLEO experiment [13], which did not observe a signal. The large data sample collected with the BESIII detector provides a good opportunity to deeply investigate these decay modes, which may shed more light on the properties of the Y(4260).

In this paper, we report on a search for $e^+e^-\to\gamma\chi_{cJ}$ ($J=0$, 1, 2) based on the large e^+e^- annihilation data samples collected with the BESIII detector at center-of-mass energies (CME) $\sqrt{s}=4.009$, 4.230, 4.260, and 4.360 GeV, where the χ_{cJ} is reconstructed by its $\gamma J/\psi$ decay mode, and the J/ψ is by its decay to $\mu^+\mu^-$. The decay $J/\psi\to e^+e^-$ is not considered in this analysis due to the high background of Bhabha events. The corresponding luminosities of the data samples at different CME used in this analysis are listed in Table 1.

Table 1. The center-of-mass energy and Luminosity of each data sample.

$\sqrt{s}$/GeV	luminosity/$\rm pb^{-1}$
4.009	482
4.230	1047
4.260	826
4.360	540

2 BESIII detector and Monte Carlo

The BESIII detector at the BEPC II collider [17] is a large solid-angle magnetic spectrometer with a geometrical acceptance of 93% of 4π solid angle consisting of four main components. The innermost is a small-cell, helium-based (40% He, 60% C_3H_8) main drift chamber (MDC) with 43 layers providing an average single-hit resolution of 135 μm. The resulting charged-particle momentum resolution for a 1 T magnetic field setting is 0.5% at 1.0 GeV/c, and the resolution on the ionization energy loss information (dE/dx) is better than 6%. The next detector, moving radially outwards, is a time-of-flight (TOF) system constructed of 5 cm thick plastic scintillators, with 176 detectors of 2.4 m length in two layers in the barrel and 96 fan-shaped detectors in the end-caps. The barrel (end-cap) time resolution of 80 ps (110 ps) provides a 2σ K/π separation for momenta up to 1.0 GeV/c. Continuing outward, we have an electromagnetic calorimeter (EMC) consisting of 6240 CsI(Tl) crystals in a cylindrical barrel structure and two end-caps. The energy resolution at 1.0 GeV is 2.5% (5%) and the position resolution is 6 mm (9 mm) in the barrel (end-caps). Finally, the muon counter consists of 1000 $\rm m^2$ of Resistive Plate Chambers in nine barrel and eight end-cap layers, which provides a 2 cm position resolution.

A GEANT4 [18] based Monte Carlo (MC) simulation software, which includes the geometric description of the detector and the detector response, is used to optimize the event selection criteria, determine the detection efficiency, and estimate the potential backgrounds. Signal MC samples of $e^+e^-\to\gamma\chi_{cJ}$ are generated for

each CME according to the electric-diplole (E1) transition assumption [19]. Effects of ISR are simulated with KKMC [20] by assuming that $\gamma\chi_{cJ}$ is produced via Y(4260) decays, where the Y(4260) is described by a Breit-Wigner function with resonance parameters from the world average [21]. For the background studies, an 'inclusive' Y(4260) MC sample equivalent to 500 pb^{-1} integrated luminosity is generated which includes the Y(4260) resonance, ISR production of the known vector charmonium states, and events driven by QED processes. The known decay modes are generated with EvtGen [19] with branching fractions set to their world average values in the Particle Data Group (PDG) [22], and the remaining events are generated with Lundcharm [23] or PYTHIA [24].

3 Event selection

Charged tracks are reconstructed in the MDC. For each good charged track, the polar angle must satisfy $|\cos\theta| < 0.93$, and the point of closest approach to the interaction point must be within ± 10 cm in the beam direction and within ± 1 cm in the plane perpendicular to the beam direction. The number of good charged tracks is required to be two with a zero net charge. Charged tracks are identified as muons if they have $E/p < 0.35$ c and $p > 1.0$ GeV/c, where E is the energy deposited in the EMC and p is the momentum measured by the MDC.

Photons are reconstructed from isolated showers in the EMC that are at least 20 degrees away from any of the charged tracks. To improve the reconstruction efficiency and the energy resolution, the energy deposited in the nearby TOF counters is included. Photon candidates are required to have energy greater than 25 MeV in the EMC barrel region ($|\cos\theta|<0.8$), and 50 MeV in the end-cap region ($0.86<|\cos\theta|<0.92$). In order to suppress electronic noise and energy deposits that are unrelated to the event, the EMC time t of the photon candidates must be in coincidence with collision events within the range $0\leqslant t\leqslant 700$ ns. At least two photon candidates in the final state are required.

To improve the momentum resolution and to reduce backgrounds, a kinematic fit with five constraints ($5C$-fit) is performed under the $e^+e^- \to \gamma\gamma\mu^+\mu^-$ hypothesis, imposing overall energy and momentum conservation and constraining the invariant mass of $\mu^+\mu^-$ to the nominal J/ψ mass. Candidates with a $\chi^2_{5C}<40$ are selected for further analysis. If more than one candidate occurs in an event, the one with the smallest χ^2_{5C} is selected. Due to the kinematics of the reaction, the first radiative photon from $e^+e^-\to\gamma\chi_{cJ}$ has a high energy while the second radiative photon from $\chi_{cJ}\to\gamma$J/ψ has a lower energy at $\sqrt{s}$=4.230, 4.260, and 4.360 GeV. The invariant mass of the low energy photon and J/ψ, $M_{\gamma J/\psi}$, is used to search for χ_{cJ} signals. However, for the data sample taken at $\sqrt{s}$ =4.009 GeV, there is an overlap of the energy distributions of the photons from $e^+e^-\to\gamma\chi_{c1,2}$ and from $\chi_{c1,2}$ decays, as shown in Fig. 1. To separate the overlapping photon spectra, the energy of photons from $\chi_{c1,2}$ decays is further required to be less than 0.403 GeV at $\sqrt{s}$=4.009 GeV.

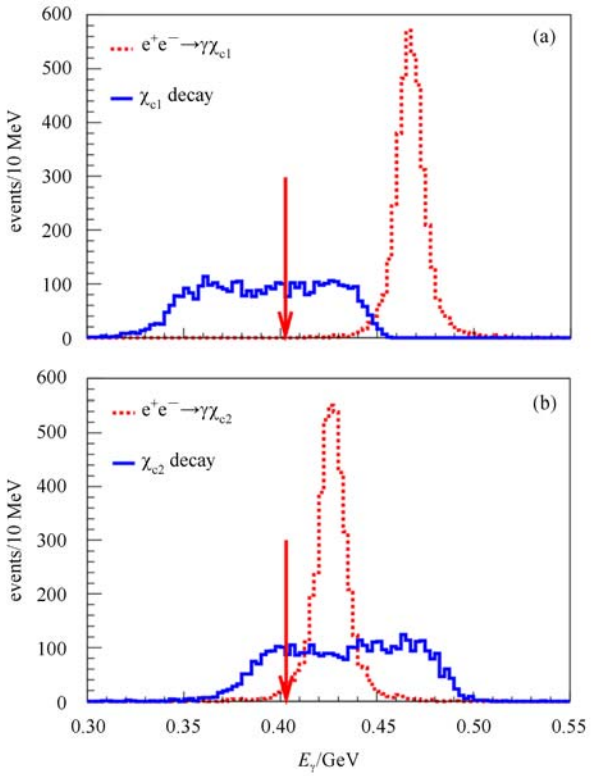

Fig. 1. The distributions of photon energies in the laboratory frame from $e^+e^- \to \gamma\chi_{c1,2}$ and from $\chi_{c1,2}$ decays in the exclusive MC samples of $e^+e^-\to\gamma\chi_{c1}$, $\chi_{c1}\to\gamma$J/ψ (a) and $e^+e^-\to\gamma\chi_{c2}$, $\chi_{c2}\to\gamma$J/ψ (b) at $\sqrt{s}$=4.009 GeV. Dashed lines stand for the first radiative photons from $e^+e^-\to\gamma\chi_{c1,2}$ and solid lines for the second radiative photons from $\chi_{c1,2}$ decays.

4 Background study

The potential backgrounds from $e^+e^- \to$ P+J/ψ, P$\to\gamma\gamma$ (P = π^0,η, or η') can be rejected by requiring $|M_{\gamma\gamma}-M_{\pi^0}|>0.025$ GeV/c^2, $|M_{\gamma\gamma}-M_{\eta}|>0.03$ GeV/c^2 and $|M_{\gamma\gamma}-M_{\eta'}|>0.02$ GeV/c^2, where $M_{\gamma\gamma}$ is the invariant mass of two selected photons. The background from $e^+e^-\to\gamma_{\rm ISR}\psi(2S)$, $\psi(2S)\to\gamma\chi_{cJ}$ is rejected by applying the $5C$ kinematic fit. After imposing all the selection criteria above, the remaining dominant background is from radiative dimuon events, which is not expected to peak in the $M_{\gamma J/\psi}$ distribution. This has been validated by a dedicated simulation study. For other remaining

backgrounds, such as $e^+e^- \to \pi^0\pi^0 J/\psi$, only 3.8 events (normalized to data luminosity) survive and can be neglected.

5 Fit to the mass spectrum

The resulting $M_{\gamma J/\psi}$ distributions, after applying the above selection criteria, at $\sqrt{s}$=4.009, 4.230, 4.260 and 4.360 GeV are shown in Fig. 2. An unbinned maximum likelihood fit of the $M_{\gamma J/\psi}$ distribution is performed to extract the numbers of χ_{cJ} signal events. In the fit, the shapes of the χ_{cJ} signals are described by double Gaussian functions, where the means and the standard deviations of the double Gaussian functions are determined from a fit to the corresponding signal MC samples at $\sqrt{s}$=4.260 GeV. These shapes are also used for the other three CME points, as the resolution varies only mildly between $\sqrt{s}$=4.009–4.360 GeV. This has been validated by MC simulation. Since the dominant background

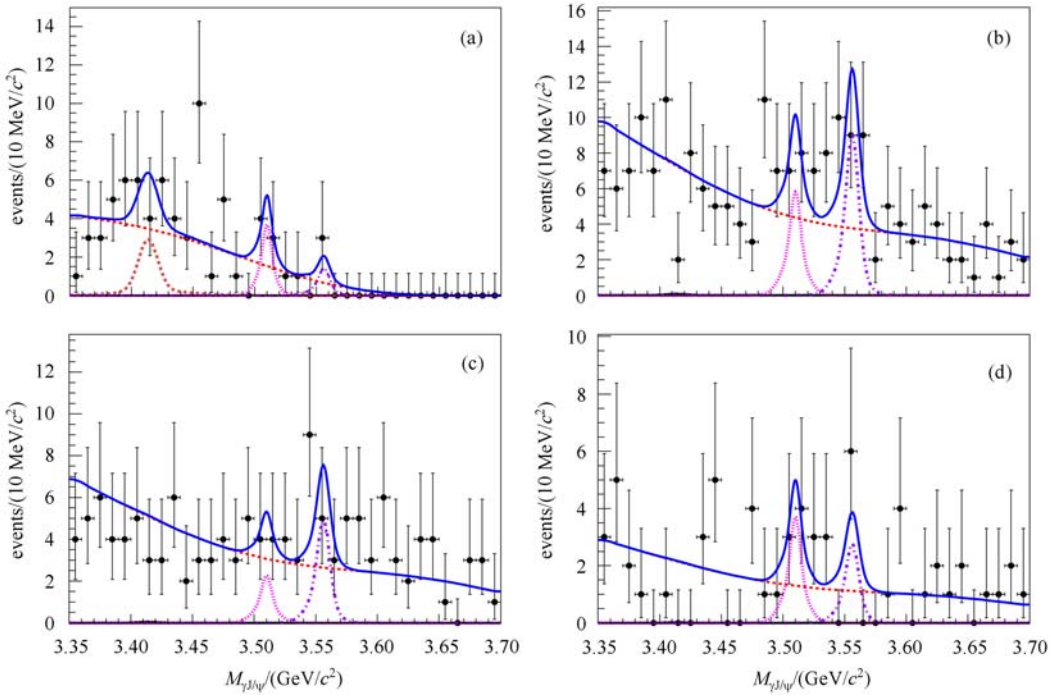

Fig. 2. The distribution of $\gamma J/\psi$ invariant mass, $M_{\gamma J/\psi}$, and fit results for data at $\sqrt{s}$=4.009 (a), 4.230 (b), 4.260 (c) and 4.360 GeV (d). The solid lines show the total fit results. The χ_{cJ} signals are shown as dashed lines, dotted lines, and dash-dotted lines, for J = 0, 1, and 2, respectively. The backgrounds are indicated by red dashed lines.

Table 2. The results on $e^+e^- \to \gamma\chi_{cJ}$ Born cross section measurement. Shown in the table are the significance σ, detection efficiency ϵ, number of signal events from the fits $N^{\rm obs}$, radiative correction factor $(1+\delta^r)$, vacuum polarization factor $(1+\delta^v)$, upper limit (at the 90% confidence level (C.L.)) on the number of signal events $N^{\rm UP}$, Born cross section $\sigma^{\rm B}$ and upper limit (at the 90% C.L.) on the Born cross section $\sigma^{\rm UP}$ at different CME points. The first uncertainty of the Born cross section is statistical, and the second systematic.

$\sqrt{s}$/GeV		$N^{\rm obs}$	significance (σ)	$N^{\rm UP}$	ϵ (%)	$1+\delta^r$	$1+\delta^v$	$\sigma^{\rm UP}$/pb	$\sigma^{\rm B}$/pb
4.009	χ_{c0}	7.0±6.6	1.6	18	36.4±0.2	0.738	1.04	179	65.0±61.3±4.2
	χ_{c1}	4.4±2.6	2.2	9	23.4±0.1			5.3	2.4±1.4±0.2
	χ_{c2}	1.8±1.7	1.5	6	8.7±0.1			18	4.7±4.4±0.6
4.230	χ_{c0}	0.2±2.3	0.0	7	37.2±0.2	0.840	1.06	26	0.7±8.0±0.1
	χ_{c1}	6.7±4.3	1.9	14	44.4±0.2			1.7	0.7±0.5±0.1
	χ_{c2}	13.3±5.2	2.9	22	42.0±0.2			5.0	2.7±1.1±0.3
4.260	χ_{c0}	0.1±1.9	0.0	5	36.7±0.2	0.842	1.06	25	0.5±8.8±0.1
	χ_{c1}	3.0±3.0	1.1	7	42.7±0.2			1.1	0.4±0.4±0.1
	χ_{c2}	7.5±3.9	2.3	14	41.7±0.2			4.2	2.0±1.1±0.2
4.360	χ_{c0}	0.1±0.7	0.0	3	32.4±0.2	0.943	1.05	23	0.7±5.0±0.1
	χ_{c1}	5.2±4.9	2.4	10	31.7±0.2			2.9	1.4±1.3±0.1
	χ_{c2}	4.4±4.5	2.0	9	30.3±0.2			5.0	2.3±2.3±0.2

Table 3. Summary of systematic uncertainties at $\sqrt{s}$=4.009, 4.230, 4.260, and 4.360 GeV(%).

$\sqrt{s}$/GeV	4.009			4.230			4.260			4.360		
sources	χ_{c0}	χ_{c1}	χ_{c2}	χ_{c0}	χ_{c1}	χ_{c2}	χ_{c0}	χ_{c1}	χ_{c2}	χ_{c0}	χ_{c1}	χ_{c2}
luminosity	1.0	1.0	1.0	1.0	1.0	1.0	1.0	1.0	1.0	1.0	1.0	1.0
tracking efficiency	2.0	2.0	2.0	2.0	2.0	2.0	2.0	2.0	2.0	2.0	2.0	2.0
photon detection	2.0	2.0	2.0	2.0	2.0	2.0	2.0	2.0	2.0	2.0	2.0	2.0
kinematic fit	0.6	0.6	0.6	0.6	0.6	0.6	0.6	0.6	0.6	0.6	0.6	0.6
branching ratio	4.8	3.6	3.7	4.8	3.6	3.7	4.8	3.6	3.7	4.8	3.6	3.7
vacuum polarization factor	0.5	0.5	0.5	0.5	0.5	0.5	0.5	0.5	0.5	0.5	0.5	0.5
χ_{cJ} mass resolution	0.3	2.0	7.4	0.0	7.7	7.8	0.0	4.3	6.5	0.0	1.1	2.0
χ_{cJ} mass	0.0	0.9	1.4	0.0	0.3	0.2	0.0	0.1	0.1	0.0	0.3	0.4
MC model	0.0	2.2	3.9	0.0	1.2	3.3	0.0	1.9	2.9	0.0	1.5	2.1
fit range	0.1	2.2	2.6	0.0	1.5	2.3	0.0	3.1	2.5	0.0	3.0	3.7
background shape	0.0	3.1	5.6	0.0	0.7	0.3	0.0	1.1	0.4	0.0	0.9	0.1
radiative correction factor	3.0	2.7	3.6	2.6	3.1	2.1	3.5	2.1	2.5	1.8	3.4	3.8
total	6.5	7.3	12.1	6.3	9.8	10.2	6.7	7.7	9.3	6.0	6.9	7.7

comes from radiative dimuon events, the corresponding MC simulation is used to represent the background shape. To reduce the effect of statistical fluctuations, the dimuon MC shape is smoothed before it is taken as the background function. Fig. 2 also shows the fitted results for the $M_{\gamma J/\psi}$ distribution at different CME. The number of fitted χ_{cJ} signal events, as well as the corresponding statistical significances (calculated by comparing the fit log likelihood values with and without the χ_{cJ} signal) at the four CME points are listed in Table 2. The same fit is applied to the sum of $M_{\gamma J/\psi}$ distributions of the four CME points. The statistical significances for χ_{c0}, χ_{c1} and χ_{c2} are found to be 1.2σ, 3.0σ and 3.4σ, respectively. The goodness of the fit is estimated by using a χ^2 test method with the data distributions regrouped to ensure that each bin contains more than 7 events. The test gives χ^2/d.o.f=39.7/32, where d.o.f is the number of degrees of freedom. As a test, we perform similar analyses to control samples from the J/ψ sideband regions, 2.917 $< M_{\mu^+\mu^-} <$ 3.057 GeV/c^2 and 3.137 $< M_{\mu^+\mu^-} <$ 3.277 GeV/c^2, by constraining the invariant mass of $\mu^+\mu^-$ to 2.987 or 3.207 GeV/c^2 in 5C-fit, and find no obvious χ_{cJ} signals.

6 Results

The Born cross section at different CME is calculated with

$$\sigma^{\rm B}(e^+e^-\to\gamma\chi_{cJ})=\frac{N^{\rm obs}}{\mathcal{L}\cdot(1+\delta^r)\cdot(1+\delta^v)\cdot\mathcal{B}\cdot\epsilon}, \qquad (1)$$

where $N^{\rm obs}$ is the number of observed events obtained from the fit, $\mathcal{L}$ is the integrated luminosity, $1+\delta^r$ is the radiative correction factor for χ_{cJ} with the assumption that the $e^+e^-\to\gamma\chi_{cJ}$ cross section follows the Y(4260) Breit-Wigner line shape [25], $1+\delta^v$ is the vacuum polarization factor [26], $\mathcal{B}$ is the combined branching ratio of $\chi_{cJ}\to\gamma J/\psi$ and $J/\psi\to\mu^+\mu^-$, and ϵ is the detection efficiency. The detection efficiencies, radiative correction factors as well as the calculated Born cross sections at different CME are shown in Table 2. The much lower efficiencies for $\chi_{c1,2}$ at $\sqrt{s}$=4.009 GeV are due to the requirement on the photon energy used to separate the overlapping photon spectra as described in Section 3.

Since the χ_{cJ} signals are not statistically significant at the individual CME points, we also give in Table 2 the upper limits on the Born cross sections at the 90% confidence level (C.L.) under the assumption that no signals are present. The upper limits are derived using a Bayesian method [21], where the efficiencies are lowered by a factor of $(1-\sigma_{\rm sys})$ to take systematic uncertainties into account.

We also perform a simultaneous fit to the $M_{\gamma J/\psi}$ distribution at $\sqrt{s}$=4.009, 4.230, 4.260, and 4.360 GeV, assuming the production cross section of $e^+e^-\to\gamma\chi_{cJ}$ at a different CME point follows the line shape of the Y(4260) state. In the fit, the line shapes of the χ_{cJ} signals and the background are the same as those in the previous fits, and the number of χ_{cJ} events at each CME point is expressed as a function of $\epsilon_{\rm c.m.}\mathcal{L}_{\rm c.m.}R_{\rm c.m.}(1+\delta^r)$, where $\epsilon_{\rm c.m.}$ and $\mathcal{L}_{\rm c.m.}$ are the detection efficiency and luminosity, respectively, and $R_{\rm c.m.}$ is the ratio of the cross section calculated with the Y(4260) line shape (a Breit-Wigner function with parameters fixed to the PDG values) at different CME points to that at $\sqrt{s}$=4.260 GeV. The corresponding fit result is shown in Fig. 3. The goodness of the fit is χ^2/d.o.f =53.3/40 and the statistical significances for χ_{c0}, χ_{c1} and χ_{c2} signals are 0σ, 2.4σ and 4.0σ, respectively. We also found that $\Gamma_{e^+e^-}\times\mathcal{B}(\Upsilon(4260)\to\gamma\chi_{c1})$ =(0.11±0.06) eV and $\Gamma_{e^+e^-}\times\mathcal{B}(\Upsilon(4260)\to\gamma\chi_{c2})$ =(0.33±0.11) eV.

7 Systematic uncertainties

The systematic uncertainties in the cross section measurements of $e^+e^-\to\gamma\chi_{cJ}$ are caused by various sources

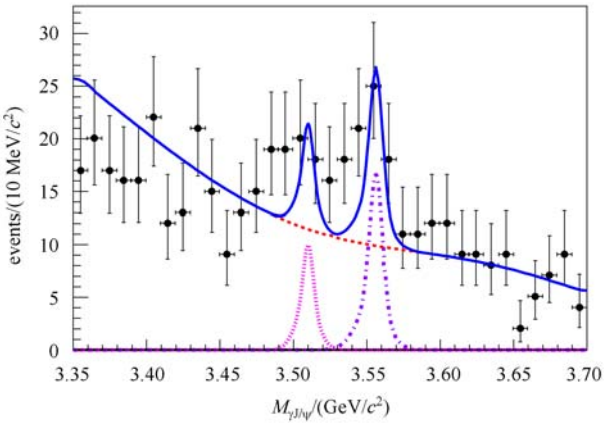

Fig. 3. Result of the simultaneous fit to $M_{\gamma J/\psi}$ distributions for all CME data sets assuming that the signals are from decays of the Y(4260). The blue solid line is the total fit result. The χ_{cJ} signals are shown as dotted line and dash-dotted line, respectively, and the background is shown as the red dashed line.

which all the channels have partially in common. The common sources of systematics include the luminosity measurement, reconstruction efficiencies for charged tracks and photons, the vacuum polarization factor, kinematic fit and branching fractions of the decay of the intermediate states. The systematic uncertainty due to the luminosity measurement is estimated to be 1.0% using Bhabha events [14]. The uncertainty related to the track reconstruction efficiency of high-momentum muons is 1.0% per track [27]. The systematic uncertainty related to the photon detection is estimated to be 1.0% per photon [14]. The systematic uncertainty due to 5C-fit is 0.6%, obtained by studying a control sample of $\psi(2S)\to\eta J/\psi$ decays. The uncertainty related to the branching fractions of χ_{cJ} and J/ψ decays are taken from the PDG [21]. The uncertainty for the vacuum polarization factor is 0.5% [26].

The other systematic uncertainties arising from the χ_{cJ} mass resolution, the shift of the χ_{cJ} reconstructed mass, the MC model, the shape of the background, the radiative correction factor and the fit range at different CME points are discussed below.

The $\psi(2S)\to\gamma\chi_{cJ}$ channel is employed as a control sample to extract the differences on the mass resolution of the χ_{cJ} signal by fitting the $M_{\gamma J/\psi}$ spectrum. The differences in the mass resolutions between data and MC are found to be 0.02%, 0.01%, 0.2% for χ_{cJ} (J =0, 1, 2). A similar fit is performed, in which the signal shapes are smeared to compensate for the mass resolution difference, and the differences on the yields of χ_{cJ} signal are taken as the systematic uncertainties due to the mass resolution.

An alternative fit is performed shifting the mean of χ_{cJ} signal shapes by one standard deviation of the PDG values, and the deviations of the signal yields to the nominal values are taken as the systematic uncertainties due to the uncertainties of the signal line shapes.

The detection efficiency is evaluated using MC samples based on the E1 transition assumption [19] for $Y(4260)\to\gamma\chi_{cJ}$. Another set of MC samples is generated where the $Y(4260)\to\gamma\chi_{cJ}$ decay is modeled using a phase space distribution, and the differences of the detector efficiencies between the two sets of MC samples are treated as systematic uncertainties from the MC model.

To estimate the systematic uncertainty related to the background shape, a control sample is selected from the data by requiring a $\mu^+\mu^-$ pair and at least one photon. An alternative background shape is then extracted by re-weighting the $\gamma\mu^+\mu^-$ invariant mass spectrum of the control sample, where the weights are the efficiency ratio of $e^+e^-\to(n\gamma)\mu^+\mu^-$ MC simulated events surviving the signal selection criteria to the same selection criteria for the control sample. A fit with the alternative background shape is performed, and the differences between the yields of χ_{cJ} signal to the nominal ones are taken as the systematic uncertainties due to the shape of the background.

The possible distortions of the Y(4260) line shape due to interference effects with nearby resonances could introduce uncertainties in the radiative correction factor $\epsilon\times(1+\delta^r)$. To estimate the related systematic uncertainties, we instead assume that $e^+e^-\to\gamma\chi_{cJ}$ are produced via $\psi(4040)$ decays at $\sqrt{s}$=4.009 GeV, $\psi(4160)$ decays at $\sqrt{s}$=4.229 and 4.260 GeV, and $\psi(4415)$ decays at $\sqrt{s}$=4.360 GeV. The variations in the factor $\epsilon\times(1+\delta^r)$ are taken as the systematic uncertainties due to the radiative correction factor.

A series of similar fits are performed in different ranges of the $M_{\gamma J/\psi}$ distribution, and the largest differences on the signal yields to the nominal values are taken as systematic uncertainties.

All the systematic uncertainties from the different sources are summarized in Table 3. The total systematic uncertainties are calculated as the quadratic sum of all individual terms.

8 Summary

Using data samples collected at CME of $\sqrt{s}$=4.009, 4.230, 4.260, and 4.360 GeV with the BESIII detector, we perform a search for $e^+e^-\to\gamma\chi_{cJ}$ (J=0, 1, 2) with the subsequent decay $\chi_{cJ}\to\gamma J/\psi$ and $J/\psi\to\mu^+\mu^-$. We find evidence for the processes $e^+e^-\to\gamma\chi_{c1}$ and $e^+e^-\to\gamma\chi_{c2}$ with statistical significances of 3.0σ and 3.4σ, respectively. No evidence of $e^+e^-\to\gamma\chi_{c0}$ is observed. The corresponding Born cross sections of $e^+e^-\to\gamma\chi_{cJ}$ at different CME are calculated and listed in Table 2. Under the assumption of the absence of χ_{cJ} signals, the upper

limits on the Born cross sections at the 90% C.L. are calculated and listed in Table 2, too. These upper limits on the Born cross section of $e^+e^-\to\gamma\chi_{cJ}$ are compatible with the theoretical prediction from an NRQCD calculation [16].

The BESIII collaboration thanks the staff of BEPCII and the IHEP computing center for their strong support.

References

1 Aubert B et al. (BABAR collaboration). Phys. Rev. Lett., 2005, **95**: 142001
2 HE Q et al. (CLEO collaboration). Phys. Rev. D, 2006, **74**: 091104(R)
3 YUAN C Z et al. (Belle collaboration). Phys. Rev. Lett., 2007, **99**: 182004
4 Lees J P et al. (BABAR collaboration). Phys. Rev. D, 2012, **86**: 051102
5 LIU Z Q et al. (Belle collaboration). Phys. Rev. Lett., 2013, **110**: 252002
6 Eichten E, Gottfried K, Kinoshita T, Lane K, YAN T. Phys. Rev. D, 1978, **17**: 3090; 1980, **21**: 203; Barnes T, Godfrey S, Swanson E S. Phys. Rev. D, 2005, **72**: 054026
7 LIU L et al. (Hadron Spectrum collaboration). JHEP, 2012, **1207**: 126
8 Ebert D, Faustov R N, Galkin V O. Phys. Lett. B, 2006, **634**: 214
9 Maiani L, Riquer V, Piccinini F, Polosa A D. Phys. Rev. D, 2005, **72**: 031502(R)
10 LIU X, ZENG X Q, LI X Q. Phys. Rev. D, 2005, **72**: 054023(R)
11 YUAN C Z, WANG P, MO X H. Phys. Lett. B, 2006, **634**: 399
12 WANG X L et al. (Belle collaboration). Phys. Rev. D, 2013, **87**: 051101(R)
13 Coan T E et al. (CLEO collaboration). Phys. Rev. Lett., 2006, **96**: 162003
14 Ablikim M et al. (BESIII collaboration). Phys. Rev. Lett., 2014, **112**: 092001
15 MA L, SUN Z F, LIU X H, DENG W Z, LIU X, ZHU S L. Phys. Rev. D, 2014, **90**: 034020
16 CHAO K T, HE Z G, LI D, MENG C. hep-ex/arXiv:1310.8597
17 Ablikim M et al. (BESIII collaboration). Nucl. Instrum. Methods A, 2010, **614**: 345
18 Agostinelli S et al. (GEANT4 collaboration). Nucl. Instrum. Methods A, 2003, **506**: 250
19 Lange D J. Nucl. Instrum. Methods A, 2001, **462**: 152; PING R G. HEP & NP, 2008, **32**: 599602
20 Jadach S, Ward B F L, Was Z. Comput. Phys. Commum., 2000, **130**: 260; Jadach S, Ward B F L, Was Z. Phys. Rev. D, 2001, **63**: 113009
21 Olive K A et al. (Particle Data Group). Chin. Phys. C, 2014, **38**: 090001
22 Beringer J et al. (Particle Data Group). Phys. Rev. D, 2012, **86**: 010001
23 PING R G. Chinese Phys. C, 2008, **32**: 599
24 Sjostrand T, Lonnblad L, Mrenna S. hep-ph/0108264
25 Kuraev E A, Fadin V S. Sov. J. Nucl. Phys., 1985, **41**: 466 [Yad. Fiz. 1985, **41**: 733]
26 Actis S et al. Eur. Phys. J. C, 2010, **66**: 585
27 Ablikim M et al. (BESIII collaboration). Phys. Rev. D, 2012, **86**: 071101